## Dispersion of the strongly correlated electron system near the Fermi level

A. Sherman

Institute of Physics, University of Tartu, Riia 142, 51014 Tartu, Estonia (November 16, 2018)

## Abstract

The reason for the appearance of two distinct bands in the photoemission of the single  $\text{CuO}_2$  plane  $\text{Bi}_2\text{Sr}_{2-x}\text{La}_x\text{CuO}_{6+\delta}$  near the Fermi level is discussed on the basis of the self-consistent solution of the two-dimensional t-J model.

PACS numbers: 74.25.Jb, 71.27.+a, 74.72.Hs, 79.60.-i

Typeset using  $\text{REVT}_{EX}$ 

Angle resolved photoemission spectroscopy data have been one of the most important sources of information about the electronic structure of the high temperature superconductors (see, e.g., Ref. 1 and references therein). One of the most interesting results obtained recently with this experimental method is the observation of two distinct emissions near the Fermi energy on Bi<sub>2</sub>Sr<sub>2-x</sub>La<sub>x</sub>CuO<sub>6+ $\delta$ </sub> in the vicinity of the ( $\pi$ , 0) point.<sup>2,3</sup> This crystal is a single CuO<sub>2</sub> layer material with sufficiently decoupled layers. Therefore the two emissions cannot be ascribed to the bilayer splitting.

Normal state photoemission spectra obtained in Ref. 3 in the optimally doped crystal with  $T_c = 29$  K are reproduced in Fig. 1(a)–(c). The measurements were performed at the temperature T = 45 K. Along the  $\Gamma M$  direction  $[\mathbf{k}_M = (\pi, 0)]$  the spectra consist of two emission bands which are well resolved for wave vectors some distance away from the Mpoint and merge to a structure which cannot be resolved into individual contributions on approaching this point. The emission band with the higher binding energy has a considerably larger halfwidth and stronger dispersion in comparison with the band with the lower binding energy.

In this Communication I would like to call attention to the fact that in many respects similar spectra were obtained<sup>4,5</sup> in the two-dimensional t-J model of the CuO<sub>2</sub> plane. In these works self-consistent calculations of the hole and magnon Green's functions were carried out for the cases from light to moderate doping with the use of the Born and different versions of the spin-wave approximations. As pointed out in these works, for moderate hole concentrations x the hole spectrum contains two dispersive features for wave vectors near the boundary of the magnetic Brillouin zone. One of these features – a narrow intensive peak slightly below (in the electron picture) the Fermi level – is connected with the so-called spin-polaron band. In a lightly doped crystal the width of this band is of the order of the exchange constant J which is much smaller than the hopping constant t of the model for parameters of cuprate perovskites. The spin-polaron bandwidth is characterized by the parameter of magnetic excitations because on the antiferromagnetic background the hole movement is accompanied by the magnon absorption and emission. The short-range antiferromagnetic ordering is retained in moderately doped crystals. In these conditions a part of the spin-polaron band is preserved near the boundary of the magnetic Brillouin zone. The second dispersive feature is a broad maximum which dispersion is characterized by the second energy parameter of the model t. The shape of this dispersion reproduces with some distortion the shape of the two-dimensional nearest-neighbor band.<sup>4,5</sup>

An example of the hole spectral function A – the imaginary part of the hole Green's function – with the two mentioned dispersive features is shown in Fig. 2 for the parameters t = 0.5 eV, J = 0.1 eV,  $x \approx 0.1$  and T = 0. The calculations<sup>4</sup> were carried out on a 20×20 lattice with the use of the spin-wave approximation<sup>6</sup> modified for short-range order. The narrow spin-polaron peak which intensity grows on approaching the M point is located near the Fermi level (its energy is taken as zero). For wave vectors near the  $\Gamma$  point two broad maxima, one below and one above the Fermi level, are seen in Fig. 2. Both of them belong to the dispersion with the characteristic energy t and appear together in the spectrum due to the broken symmetry implied in the spin-wave approximation. In the used magnetic Brillouin zone, which is half as much as the usual one, the spectral function contains features corresponding to two points of the usual Brillouin zone. These points are connected by the antiferromagnetic wave vector  $(\pi, \pi)$ . The experimental photoemission spectrum can be modelled by the above spectral function convoluted with the Gaussian of an appropriate width for the experimental resolution and cut off by the Fermi distribution function. The spectra obtained in this way for three wave vectors are shown in the right panel of Fig. 1. In accord with the experimental conditions of Ref. 3 in these calculations the width of the Gaussian and the temperature in the Fermi distribution were set equal to 20 meV and 45 K, respectively. In spite of some differences in relative intensities and widths of the spectral features, the calculated photoemission spectrum has the same structure as the experimental spectrum<sup>3</sup> with two spectral features (only the foot of the spin-polaron peak is shown on the right panel of Fig. 1 to demonstrate more clearly the maximum or shoulder with a larger binding energy and smaller peak intensity). The experimental and calculated dispersions of the two spectral features are compared in Fig. 3. As is seen from the figure, the experimental and calculated dispersions are similar and the binding energies are of the same order of magnitude.

In the experiment, the splitting of the photoemission band was observed along the  $\Gamma M$  direction and was not detected near the  $(\pi/2, \pi/2)$  point.<sup>3</sup> The comparison of the calculated photoemission spectra for  $\mathbf{k} = (0.6\pi, 0)$  and  $(\pi/2, \pi/2)$  is given in Fig. 4. The spectra were obtained in the same way and for the same parameters as for the right panel of Fig. 1. As can be seen from Fig. 4, the broad spectral feature reveals itself much more clearly at  $(0.6\pi, 0)$ . This is connected with the fact that near  $(\pi/2, \pi/2)$  central frequencies of the spin-polaron peak and the broad maximum are close. In this region of the Brillouin zone the spin-polaron peak touches the Fermi level and the broad maximum crosses it. The Fermi surface of the 2D *t-J* model is shown in Fig. 5 for the underdoped case.<sup>5</sup>

Recently<sup>7</sup> two dispersive features were resolved near the Fermi level in photoemission of the underdoped and optimally doped  $Bi_2Sr_2CaCu_2O_{8+\delta}$  with two  $CuO_2$  planes in the unit cell.<sup>8</sup> In Ref. 7 this splitting of the photoemission band was connected with a coupling between adjacent  $CuO_2$  planes. Since energy distribution curves and values of the band splitting in that work are similar to those observed in the single  $CuO_2$  plane  $Bi_2Sr_{2-x}La_xCuO_{6+\delta}$ , another possible mechanism of the band splitting in  $Bi_2Sr_2CaCu_2O_{8+\delta}$  – the above-discussed peculiarity of the spectrum of the 2D strongly correlated system – has to be also taken into account. It counts in favour of this latter mechanism that the Fermi surface obtained in Ref. 7 (see Fig. 1g there) is very close to the Fermi surface in Fig. 5.

In summary, it was demonstrated that the two dispersive features in the hole spectral function of the two-dimensional t-J model are similar to the features observed in the photoemission spectrum of the single CuO<sub>2</sub> plane Bi<sub>2</sub>Sr<sub>2-x</sub>La<sub>x</sub>CuO<sub>6+ $\delta$ </sub>. Thus, this peculiarity of the spectrum of the strongly correlated system can be considered as a possible reason for the photoemission band splitting in this crystal.

## REFERENCES

- <sup>1</sup> A. Damascelli, D. H. Lu, and Z.-X. Shen, J. Electron Spectr. Relat. Phenom. **117-118**, 165 (2001).
- <sup>2</sup> R. Manzke, R. Müller, C. Janowitz, M. Schneider, A. Krapf, and H. Dwelk, Phys. Rev. B **63**, R100504 (2001).
- <sup>3</sup>C. Janowitz, R. Müller, L. Dudy, A. Krapf, R. Manzke, C. Ast, and H. Höchst, condmat/0107089.
- <sup>4</sup> A. Sherman and M. Schreiber, Physica C **303**, 257 (1998); in: "Studies of High Temperature Superconductors", vol. 27, p. 163 (Nova Science Publishers, New York, 1999), ed. A. V. Narlikar; cond-mat/9808087.
- <sup>5</sup> A. Sherman and M. Schreiber, Phys. Rev. B **50**, 12887 (1994); **55**, R712 (1997); A. Sherman, Phys. Rev. B **55**, 582 (1997).
- <sup>6</sup> M. Takahashi, Phys. Rev. B **40**, 2494 (1989); S. Tang, M. E. Lazzouni and J. E. Hirsch, Phys. Rev. B **40**, 5000 (1989).
- <sup>7</sup>Y.-D. Chuang, A. D. Gromko, A. V. Fedorov, Y. Aiura, K. Oka, Y. Ando, D. S. Dessau, cond-mat/0107002.
- <sup>8</sup> Earlier the photoemission band splitting was observed in overdoped  $Bi_2Sr_2CaCu_2O_{8+\delta}$ , see D. L. Feng, N. P. Armitage, D. H. Lu, A. Damascelli, J. P. Hu, P. Bogdanov, A. Lanzara, F. Ronning, K. M. Shen, H. Eisaki, C. Kim, Z.-X. Shen, J.-I. Shimoyama, and K. Kishio, Phys. Rev. Lett. **86**, 5550 (2001). Our calculations cannot be compared with these results because the spin-wave approximation is not applicable for the overdoped case.

## FIGURES

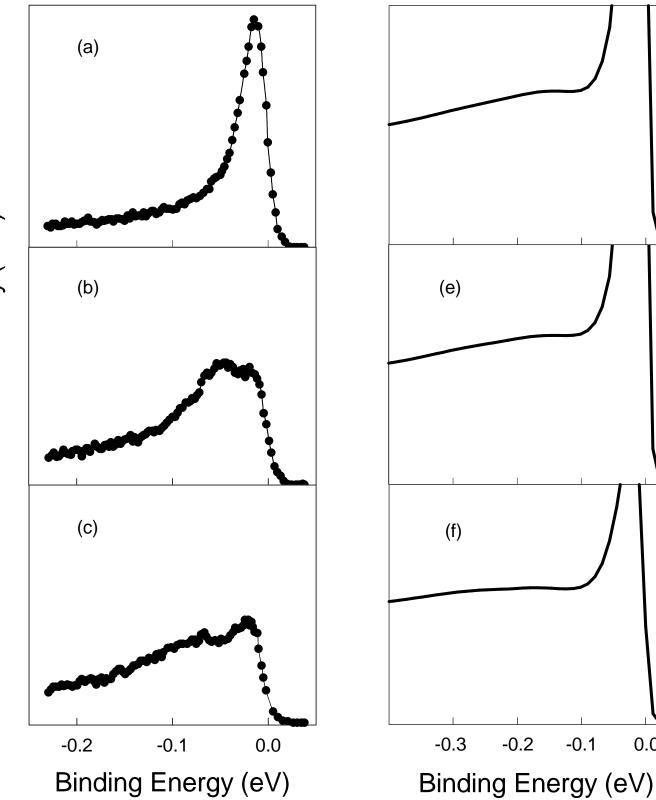
FIG. 1. Left panel: Normal state photoemission spectra of the optimally doped  $Bi_2Sr_{2-x}La_xCuO_{6+\delta}$  ( $T_c = 29$  K, T = 45 K) for  $\mathbf{k} = (0.83\pi, 0)$  (a),  $(0.69\pi, 0)$  (b), and  $(0.62\pi, 0)$  (c).<sup>3</sup> Right panel: Normal state photoemission spectra in the 2D *t-J* model for  $\mathbf{k} = (0.8\pi, 0)$  (d),  $(0.7\pi, 0)$  (e), and  $(0.6\pi, 0)$  (f). The spectra were obtained from spectral functions self-consistently calculated<sup>4</sup> for the hole concentration  $x \approx 0.1$  in a  $20 \times 20$  lattice. The spectral functions were convoluted with Gaussian with the width of 20 meV to model experimental resolution and cut off with the Fermi distribution with T = 45 K. The hopping and exchange parameters of the model are t = 0.5 eV and J = 0.1 eV.

FIG. 2. The hole spectral function of the 2D t-J model along the  $(0,0) - (\pi,0)$  direction of the Brillouin zone. The self-consistent calculations<sup>4</sup> were carried out on a 20×20 lattice for the parameters t = 0.5 eV, J = 0.1 eV,  $x \approx 0.1$  and T = 0. The Fermi energy is taken as zero of energy.

FIG. 3. (a) The dispersions of the two features in the photoemission spectrum of  $Bi_2Sr_{2-x}La_xCuO_{6+\delta}$  (the dispersions were derived in Ref. 3 by fitting the experimental spectra by two Lorentzians convoluted with a Gaussian to imitate the experimental resolution and cut off by the Fermi distribution). (b) The dispersions of the maxima in the spectral function in Fig. 2.

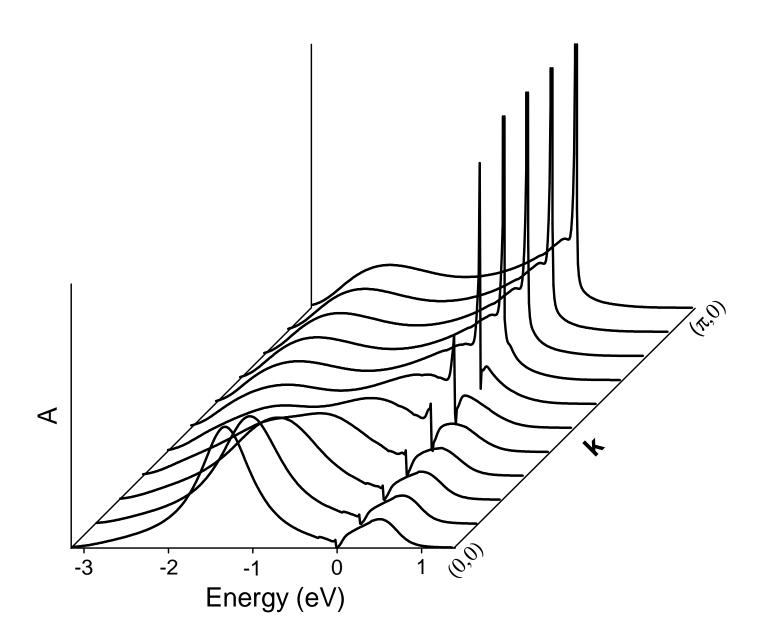
FIG. 4. The photoemission spectra in the *t*-*J* model for  $\mathbf{k} = (0.6\pi, 0)$  (solid line) and  $(\pi/2, \pi/2)$  (dashed line). The spectra were obtained in the same way and for the same parameters as for the right panel of Fig. 1.

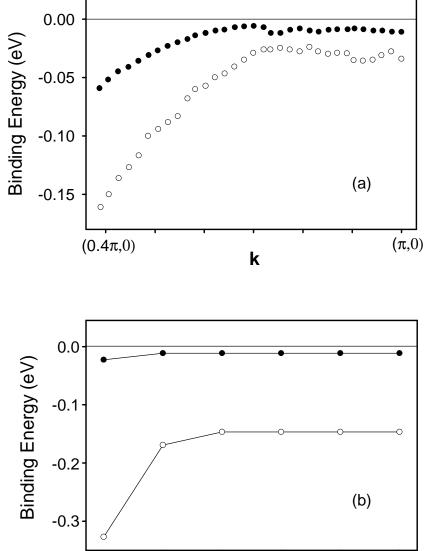
FIG. 5. The Fermi surface of the 2D t-J model for the underdoped case.<sup>5</sup> The solid segments along the boundary of the magnetic Brillouin zone are formed by points where the spin-polaron band touches the Fermi level. It is crossed by the broader dispersive feature along the dashed curves.



0.0

Normalized Intensity (a.u.)





k

(π,0)

**(**0.5π,0)

